Scripta Materialia 112 (2016) 101–105

Contents lists available at ScienceDirect

Scripta Materialia

journal homepage: www.elsevier.com/locate/scriptamat

Effect of charge redistribution factor on stacking-fault energies of Mg-based binary alloys

Y.F. Wu [a], S. Li [a,*], Z.G. Ding [a], W. Liu [a], Y.H. Zhao [a], Y.T. Zhu [a,b,*]

[a] Nano Structural Materials Center, School of Materials Science and Engineering, Nanjing University of Science and Technology, Nanjing 210094, Jiangsu, China
[b] Department of Materials Science and Engineering, North Carolina State University, Raleigh, NC 27695, USA

ARTICLE INFO

Article history:
Received 25 June 2015
Received in revised form 17 August 2015
Accepted 12 September 2015
Available online 27 September 2015

Keywords:
Magnesium alloys
First-principles calculations
Stacking-fault energies
Suzuki segregation
Charge redistribution factor

ABSTRACT

The energies of deformation fault (I_2) and twin-like fault (T_2) of thirteen binary Mg alloys were studied using density functional theory. It is shown that the faulted regions are energetically favorable for solute segregation, and the reduction of stacking-fault energy (SFE) was caused by charge redistribution. We define a charge redistribution factor, F, to quantify the solute-induced charge redistribution. An analytical model was established to calculate SFE from F.

1. Introduction

Magnesium (Mg) alloys are extensively used in automotive, aerospace and biomedical industries, thanks to their super strength to weight ratio, abundance and biodegradability [1]. However, their limited ductility and workability at room temperature have become a bottleneck for many applications. Therefore, designing new Mg alloys with improved strength and ductility has become critically important.

Stacking-fault energy (SFE) is a critical intrinsic material parameter that significantly affects the plastic deformation behavior and mechanical properties for metals [2]. For example, low SFE has been reported to enhance both strength and ductility of hexagonal close-packed (hcp) metals by the formation of high-density of stacking faults [3,4]. The stacking fault approach to increase the strength and ductility is especially important for nanostructured metals since deformation twinning, another effective approach that is effective in face-centered cubic metals, is no longer available for hcp metals when their grain sizes are very small [5,6]. The lower basal-plane SFE was also found to facilitate the formation of a long-period-stacking-ordered (LPSO) structure [7], which significantly strengthens Mg alloys. These studies clearly indicate the advantages of reducing SFEs of Mg alloys in improving the mechanical properties of hcp Mg alloys.

The addition of alloying elements is an effective approach for modifying SFEs of Mg alloys [8,9]. Suzuki [10] reported that solute atoms were easy to segregate to SFs, and this prediction has been later experimentally confirmed [11–13]. Such segregation stabilizes SF configurations and dramatically pins dislocation motion, which leads to further strengthening [14]. Despite numerous density functional theory (DFT) studies on the SFEs of Mg-based binary alloys [15–21], a definitive relationship between SFE and the electronic structure of solute atoms has not yet been established. The Suzuki effect suggests that the solute–SF chemical interaction is a dominant factor to cause change in SFE [22], while the underlying physical mechanism still remains unclear.

In this paper, we carried out DFT calculations on the SFEs of thirteen Mg-X systems (X = Cs, Ca, Sr, Sc, Y, La, Ti, Zr, Zn, Al, Ga, Sn, and Pb), and probed the physical mechanism of solute effect on SFE. It is found that the faulted regions are energetically favorable for solute segregation, and the dominant factor for the reduction of SFEs is the charge redistribution surrounding the solute atoms. In order to quantify the charge redistribution induced by solute atoms, a new parameter called charge redistribution factor, F, is defined. An analytical model is developed to describe the relationship between F and SFE, which agrees well with the results from the DFT calculations.

Two intrinsic basal-plane stacking faults, i.e. deformation fault (I_2) and twin-like fault (T_2), were studied in this paper. Instead of the *slab shearing* method [15–21], we adopted the *alias shearing* method [22] to simulate the shearing process that generates SFs. We employed a $(2 \times 3 \times 6)$ supercell with 12 layers and 12 atoms in each layer. The lattice vectors of this orthorhombic supercell are $e_1 = [1\bar{1}00]$, $e_2 = [11\bar{2}0]$, $e_3 = [0001]$. As shown in Fig. 1, I_2 (…ABA$\dot{B}\dot{C}$ACA…) is formed by shearing

* Corresponding authors at: Nano Structural Materials Center, School of Materials Science and Engineering, Nanjing University of Science and Technology, Nanjing 210094, Jiangsu, China.
E-mail addresses: lishuang@njust.edu.cn (S. Li), ytzhu@ncsu.edu (Y.T. Zhu).

http://dx.doi.org/10.1016/j.scriptamat.2015.09.023
1359-6462/

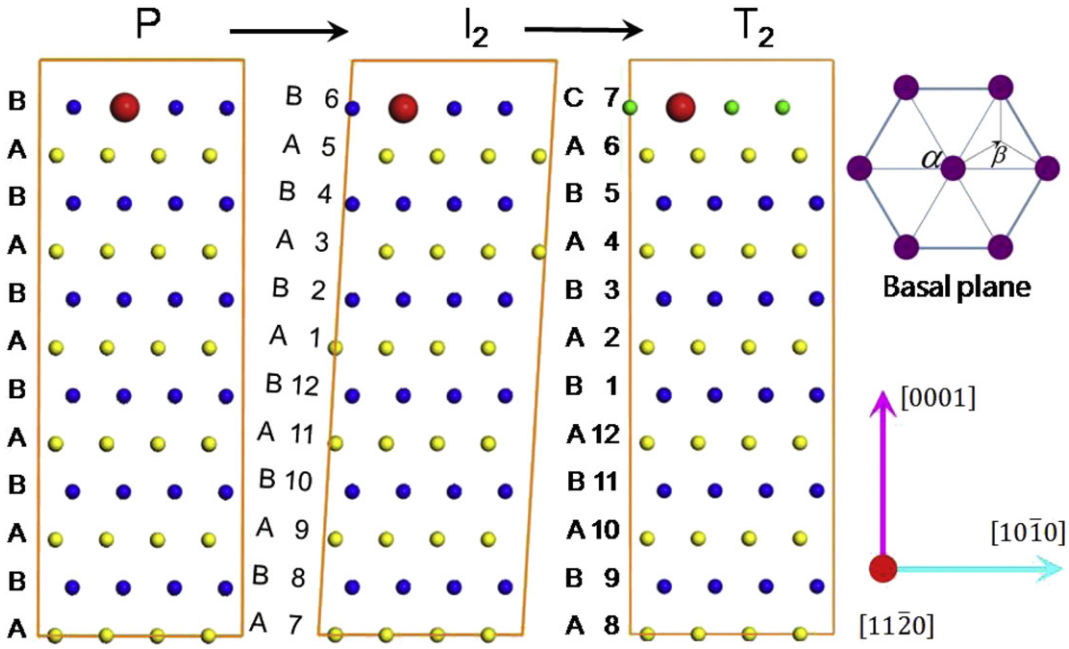

Fig. 1. The schematic illustration of pristine, I_2 and T_2 configurations. The letters A, B and C represent (0001) planes with different stacking sequences of the hcp Mg lattice, which are highlighted in yellow, blue and green solid balls respectively. The substitutional position of solutes is marked by the bigger red solid ball. The corresponding basis vectors and the shearing path in accordance with a Shockley partial ($a \rightarrow \beta$) are labeled on the right.

the lattice frame along a Shockley partial, while T_2 (…ABA$\dot{B}$C$\dot{B}$ABA…) is a competing low energy defect structure, and it has mirror symmetry about the faulted plane. For more details, refer to Refs. [22]. In this study, DFT calculations were performed using the Vienna Ab-initio Simulation Package (VASP) [23]. The generalized-gradient approximation (GGA) with Pardew–Burke–Ernzerhof (PBE) parameterization for exchange correction function was adopted [24]. The cut-off energy for plane wave basis sets was 400 eV. The *k*-points were meshed by $5 \times 5 \times 2$ *Γ*-centered grids [25]. The atomic positions were fully relaxed along all directions by first-order Methfessel–Paxton [26] smearing method with the width $\sigma = 0.2$ eV. Then the accurate system energy was obtained by Blöchl tetrahedral correction. The optimized lattice constants $a = 3.191$ Å and $c/a = 1.628$ perfectly agrees with the experimental values [27].

To study the Suzuki effect, the layer-by-layer relative energy was plotted in Fig. 2 to clarify the energetically favorable substitutional positions for solutes in Mg-based binary alloys. Here, the SF regions were defined as layers 6–7 for I_2 and layers 6–8 for T_2. We took the energy of layer 7 as 0 eV, as such the relative energies with respect to layer 7 of different binary systems share the same reference level. The segregation of solutes experienced different behaviors in I_2 and T_2 in terms of their preferential substitutional positions. Specifically, for I_2, all the thirteen solute atoms are attracted to the faulted layer 6 or 7 and stabilize the faulted configuration, as shown in Fig. 2(a). All solutes except Zn need to overcome an energy barrier to diffuse to layer 1 from the faulted layer 6, which indicates a difficulty for the solute atoms to diffuse away from the faulted region, i.e. a stable segregation is formed in the faulted region. Zn is supposed to distribute randomly in the faulted lattice since there is no obvious energy barrier for it to diffuse away from the faulted region of I_2. Remarkably, the deviation of Cs from the SF region is the most difficult among all considered elements. A larger energy barrier corresponds to a stronger solute-SF interaction. The degree of solute–SF (I_2) interaction is sequenced by: Cs > La > Y (Sr) > Sn (Pb) > Al (Sc, Zr) > Ca > Ti > Ga > Zn. For all considered Mg-X systems, the energy barriers for T_2 are systematically smaller than those for I_2, as illustrated in Fig. 2(b). However, it is interesting to find that Ti and Zr tend to segregate in the faulted layer 6 or 8 while the others prefer the pristine layer 7 in T_2. It is also clear that Zn, Al and Ga have no obvious energy barrier, which manifests a random distribution of these elements in the faulted lattice. The corresponding comparison on the solute-SF (T_2) interaction is then concluded as: Cs > La > Sr > Ca > Y > Ti > Zr > Sn (Pb) > Sc > Al (Ga) > Zn.

After determining the solute position in the faulted lattice, the SFE is derived by the following equation:

$$\gamma_x = \frac{E_x - E_P}{S} \tag{1}$$

where *x* represents I_2 or T_2. E_x and E_p denote the total energy of the faulted and the pristine supercell, respectively. *S* is the faulted area of the supercell. The calculated I_2 and T_2 SFEs for pure Mg and Mg-X systems are summarized in Table 1. The data indicate that the additions of Zn, Al, Ga, Sn and Pb are capable of lowering the SFEs by about 1–5 mJ m^{-2}. La, Ca, Sr, Y, La, and Zr can decrease the SFEs by more than 5–10 mJ m^{-2}. Cs and La lead to a dramatic reduction of the SFEs by over 15–20 mJ m^{-2}. Additionally, the previous DFT calculations by *alias shearing* are also available in Table 1 for comparison, the difference come from the different doping concentrations and the distance of the stacking faults after periodic repeat.

Wang et al. found that the SFE of pure Mg was proportional to the difference of the maximum deformation charge density between fault and non-fault planes [28]. Han et al. [29] confirmed the important contribution of charge redistribution in the changes of the generalized stacking-fault energy (GSFE). The charge distribution diagrams of pure Mg, Mg–Cs, Mg–Ca, Mg–Sc, Mg–Ti, Mg–Zn, Mg–Al and Mg–Sn systems in respect to pristine lattices obtained from the DFT calculations are shown in Fig. 3. As seen from pristine lattice of the pure Mg system, Mg ions are combined by perfect pseudo-atom (p-a) bonds that should be shaped as hexagonal when viewed from the [0001] direction. These p-a bonds are completely destroyed in the faulted layer, which gives rise to SFE.

Solute atoms disturb the electronic environment and strain field of matrix atoms [30], thus, the solute-induced charge redistribution would play a significant role in determining SFEs. Therefore, we assumed

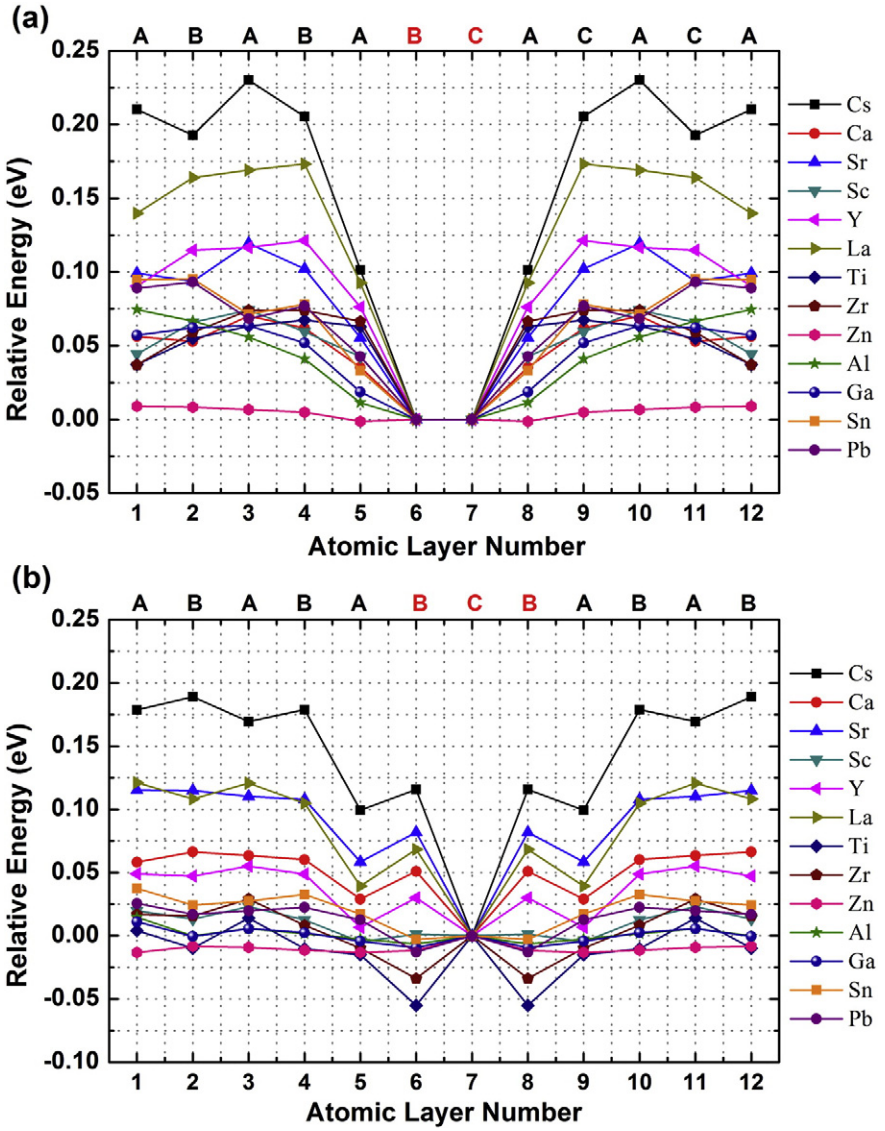

Fig. 2. The layer-by-layer energy mappings for (a) I_2 and (b) T^2 of the calculated 13 Mg-based binary alloys. The stacking fault (SF) regions are highlighted in red.

that the SFE-reduction in Mg-X binary alloys mainly depends on the disturbance of p-a bonds in the pristine lattice by the solutes. In another word, the solute-induced charge redistribution will predominantly influence the term E_p in Eq. (1), while its influence on the term E_x has been negligible because of the nonexistence of p-as in the faulted layer. The assumption is rough, according to the assumption, it can be concluded that SFEs of I_2 and T_2 in a Mg-X system will simultaneously increase or decrease, which agrees well with the results from table I.

Table 1
The SFEs mJ m^{-2} of I_2 and T_2 of pure Mg and 13 Mg-X systems (X = Cs, Ca, Sr, Sc, Y, La, Ti, Zr, Zn, Al, Ga, Sn, and Pb) along with their core and outermost charges, ionic radii and values of F in terms of Eq. (3).

System	I_2-SFE		T_2-SFE		Outermost charge	Ionic radius	F
Pure-Mg	30.0	26.1[a]	40.0	37.1[a]	2	0.49	0
Mg–Cs	4.6		13.4		1	1.67	14.59
Mg–Ca	21.8	24.5[a]	28.8	33.3[a]	2	0.99	0.75
Mg–Sr	19.0	20.2[a]	22.4	27.4[a]	2	1.12	4.53
Mg–Sc	24.4	24.9[a]	35.0	36.9[a]	3	0.73	0.14
Mg–Y	19.2	22.9[a]	31.0	33.5[a]	3	0.89	2.14
Mg–La	15.3	19.9[a]	22.6	25.5[a]	3	1.06	5.4
Mg–Ti	19.5	30.4[a]	31.5	41.8[a]	4	0.53	0.01
Mg–Zr	21.2	30.2[a]	32.3	40.8[a]	4	0.72	0.94
Mg–Zn	26.2	25.5[a]	37.6	37.2[a]	12	0.60	0
Mg–Al	29.7	24.8[a]	37.1	36.0[a]	3	0.39	0.03
Mg–Ga	28.5		36.5		13	0.47	0.01
Mg–Sn	28.1	23.0[a]	34.3	33.3[a]	14	0.69	0.14
Mg–Pb	27.6		33.8		28	0.77	0.52

[a] Ref. [22].

Basing on the above discussion, we hypothesize that an increase in charge redistribution leads to a decrease in SFE. As shown in the case of Mg–Cs system (Fig. 3), Cs atom expels the surrounding charge away from itself, and the p-a bonds around Cs are destroyed completely, which leads to the extremely reduced SFEs. In contrast, p-a bonds around Ca, Sc and Ti atoms are only partially destroyed, so that the SFEs do not decrease notably. The p-a bonds around Al, Zn and Sn are almost fully retained, thus their SFEs do not change much.

In order to quantify the solute-induced charge redistribution, we define a charge redistribution factor, F. This factor quantifies the charge density between the solute and the surrounding Mg atoms that disturbs the p-a bonds. The expression of F is proposed based on the assumption that two adjacent atoms are considered as a system, ions core denotes the positive center, and valence electrons denote the negative center. As such, the interactions between two Mg atoms are symmetric and the positive and the negative charge centers are completely overlapped, which generates a perfect p-a bond. However, for a Mg atom and a

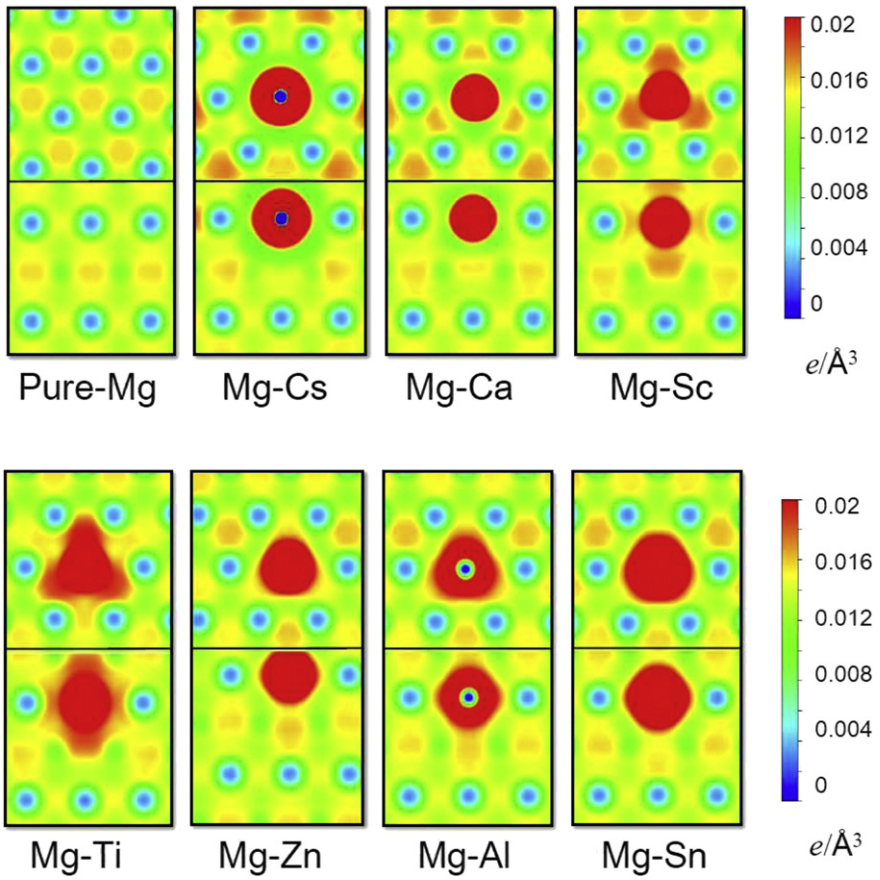

Fig. 3. The charge distribution diagrams of the pristine lattices of pure Mg. Mg–Cs, Mg–Ca, Mg–Sc, Mg–Ti, Mg–Zn, Mg–Al, and Mg–Sn systems. Up and down sides of a single box are the cross planes perpendicular to e3 and e1 respectively.

solute atom, this interaction is deemed as asymmetrical and the charge centers are separated, which leads to the deformation of a perfect p-a bond. Together with the assumption that the charge redistribution predominantly affects SFEs and only the nearest-neighbor Mg atoms around a solute atom are taken into account, the F is generalized as:

$$F = \sqrt{\frac{nq}{(1+\alpha)(1+\beta)}}\left|\frac{(\beta-\alpha)l}{(1+\alpha)(1+\beta)}+\frac{R-r\beta}{1+\beta}\right|^3 \quad (2)$$

where n and q are the outermost and the nuclear charges of a Mg atom, respectively; α and β denote the nuclear and the outermost charge ratios of Mg and solute atom X, respectively; r and R manifest the ionic radii of Mg^{2+} and X^{p+} (p is the number of the generally largest valence charge of element X); l is the lattice parameter (3.19 Å) of pure Mg. $\sqrt{\frac{nq}{(1+\alpha)(1+\beta)}}$ and $\left|\frac{(\beta-\alpha)l}{(1+\alpha)(1+\beta)}+\frac{R-r\beta}{1+\beta}\right|^3$ describe the intensity of electronic center and the distance of the positive and negative center, respectively.

The relative reduction of SFE $\Delta\gamma_x/\gamma_0$ has the relationship with F ($x = I_2, T_2$) as follows:

$$\frac{\Delta\gamma_x}{\gamma_0} = 1-\exp\left(-\sqrt{0.08F}\right) \quad (3)$$

where $\Delta\gamma_x$ is the energy difference between the SFEs of pure Mg and Mg-X systems, and γ_0 is the SFE of pure Mg. The fitting curve of $\Delta\gamma_x/\gamma_0$ and F is mapped out in Fig. 4. It is obvious that all the solutes except Ti and Cs show a nearly perfect compliance with the fitting curve. In light of Eq. (1), the value of E_x and E_p determine the SFE value, the effect of solute atoms and type of stacking fault on E_x are neglected in our model, which induces the deviation. The large discrepancy of Ti and Cs for I_2 SFE is probably related to special charge distribution energy according to a bond orientation model [31]; bond critical point (bcp) bonds emerge between the Mg atoms nearest or the next-nearest Ti and Cs.

In summary, all of the thirteen calculated elements can be stabilized at the SF regions, which demonstrate an approximately universal Suzuki segregation process. The disturbance of the p-a bonds in the pristine lattice of Mg-X causes the reduction of SFEs. F was defined to quantify

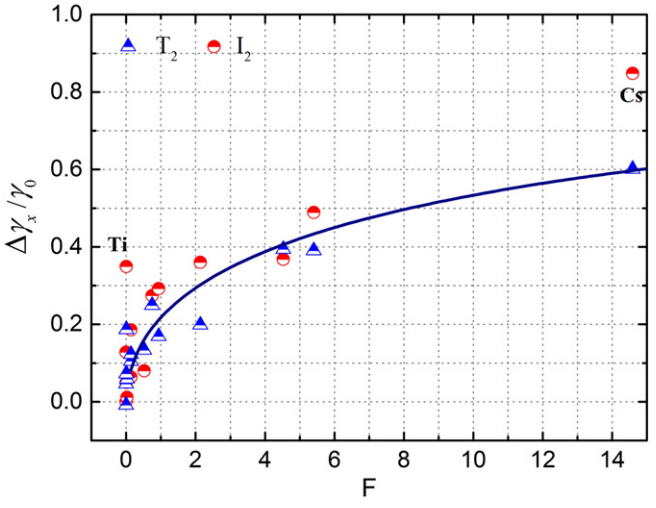

Fig. 4. The fitting curve of vs $\Delta\gamma_x/\gamma_0$ F, x = I2 and T2. SFEs of I2 and T2 are marked by red solid circles and blue solid triangle respectively. Ti and Cs are separately marked.

the solute-induced charge redistribution, and $\Delta\gamma_x/\gamma_0$ increases with F monotonously, e.g. a smaller value of SFE corresponds to a larger F value.

Acknowledgments

The authors appreciate the discussions with S.L. Shang. The authors gratefully acknowledge the financial supports of Program for New Century Excellent Talents from Chinese Ministry of Education, National Natural Science Foundation of China (51225102 and 2012CB932203) and the 8th "Liu Da Ren Cai Gao Feng" (B932203) from Jiangsu Province, China.

References

[1] T.M. Pollock, Science 328 (2010) 986.
[2] V. Vitek, Philos. Mag. 18 (1968) 773.
[3] W.W. Jian, G.M. Cheng, W.Z. Xu, C.C. Koch, Q.D. Wang, Y.T. Zhu, S.N. Mathaudhu, Appl. Phys. Lett. 103 (2013) 133108.
[4] W.W. Jian, G.M. Cheng, W.Z. Xu, H. Yuan, M.H. Tsai, Q.D. Wang, C.C. Koch, Y.T. Zhu, S.N. Mathaudhu, Mater. Res. Lett. 1 (2013) 61.
[5] Y.T. Zhu, X.Z. Liao, X.L. Wu, Prog. Mater. Sci. 57 (2012) 1.
[6] X.L. Wu, K.M. Youssef, C.C. Koch, S.N. Mathaudhu, L.J. Kesckes, Y.T. Zhu, Scr. Mater. 64 (2011) 213.
[7] E. Abe, Y. Kawamura, K. Hayashi, A. Inoue, Acta Mater. 50 (2002) 3845.
[8] S. Ganeshan, S.L. Shang, Y. Wang, Z.K. Liu, Acta Mater. 57 (2009) 3876.
[9] J.A. Yasi, L.G. Hector Jr., D.R. Trinkle, Acta Mater. 58 (2010) 5704.
[10] H. Suzuki, Sci. Rep. Res. Inst. Tohoku Univ. A 4 (1952) 455.
[11] J.F. Nie, Y.M. Zhu, J.Z. Liu, X.Y. Fang, Science 340 (2013) 957.
[12] Z.Q. Yang, M.F. Chisholm, G. Duscher, X. Li, S. Ma, J. Pennycook, Acta Mater. 61 (2013) 350.
[13] H. Zhou, G.M. Cheng, X.L. Ma, W.Z. Xu, S.N. Mathaudhu, Q.D. Wang, Y.T. Zhu, Acta Mater. 95 (2015) 20.
[14] J. Zhang, Y.C. Dou, Y. Zheng, Scr. Mater. 80 (2014) 17.
[15] J. Zhang, Y.C. Dou, G.B. Liu, Z.X. Guo, Comput. Mater. Sci. 79 (2013) 564.
[16] M. Muzyk, Z. Pakiela, K.J. Kurzydlowski, Scr. Mater. 66 (2012) 219.
[17] Q. Zhang, T.W. Fan, L. Fan, B.Y. Tang, L.M. Peng, W.J. Ding, Intermetallics 29 (2012) 21.
[18] L. Ma, R.K. Pan, T.W. Fan, B.Y. Tang, L.M. Peng, W.J. Ding, Comput. Mater. Sci. 69 (2013) 168.
[19] A. Datta, U.V. Waghmare, U. Ramamurty, Acta Mater. 56 (2008) 2531.
[20] C. Wang, H.Y. Zhang, H.Y. Wang, G.J. Liu, Q.C. Jiang, Scr. Mater. 69 (2013) 445.
[21] X.Y. Cui, H.W. Yen, S.Q. Zhu, R.K. Zheng, S.P. Ringer, J. Alloy Compd. 568 (2014) 656.
[22] S.L. Shang, W.Y. Wang, B.C. Zhou, Y. Wang, K.A. Darling, L.J. Kecskes, S.N. Mathaudhu, Z.K. Liu, Acta Mater. 67 (2014) 168.
[23] G. Kresse, J. Hafner, Phys. Rev. B 48 (1993) 13115.
[24] J.P. Perdew, Kieron Burke, Matthias Ernzergof, Phys. Rev. Lett. 77 (1996) 3865.
[25] H.J. Monkhorst, J.D. Pack, Phys. Rev. B 13 (1976) 5188.
[26] M. Methfessel, A.T. Paxton, Phys. Rev. B 40 (1989) 3616.
[27] L. Wen, P. Chen, Z.F. Tong, B.Y. Tang, L.M. Peng, W.J. Ding, Eur. Phys. J. B 72 (2009) 397.
[28] W.Y. Wang, S.L. Shang, Y. Wang, K.A. Darling, S.N. Mathaudhu, X.D. Hui, Z.K. Liu, Chem. Phys. Lett. 551 (2012) 121.
[29] J. Han, X.M. Su, Z.H. Jin, Y.T. Zhu, Scr. Mater. 64 (2011) 693.
[30] M. Yuasu, M. hayashi, M. Mabuchi, Y. Chino, Acta Mater. 65 (2014) 207.
[31] N. Chetty, M. Weinert, Physic. Rev. B 56 (1997) 1829.